Magnetic Resonance Imaging 33 (2015) 1306–1313

Contents lists available at ScienceDirect

Magnetic Resonance Imaging

journal homepage: www.mrijournal.com

Global signal regression has complex effects on regional homogeneity of resting state fMRI signal

Zhao Qing [a], Zhangye Dong [a], Sufang Li [b], Yufeng Zang [c,d], Dongqiang Liu [c,d,*]

[a] National Key Laboratory of Cognitive Neuroscience and Learning, Beijing Normal University, Beijing, China
[b] Neuroimage Research Branch, National Institute of Drug Abuse, National Institute of Health, Baltimore, MD, USA
[c] Center for Cognition and Brain Disorders, Hangzhou Normal University, Hangzhou, China
[d] Zhejiang Key Laboratory for Research in Assessment of Cognitive Impairments, Hangzhou, China

ARTICLE INFO

Article history:
Received 24 May 2013
Revised 11 May 2015
Accepted 27 July 2015

Keywords:
Resting state fMRI
Regional homogeneity
Global signal regression
Eyes open
Eyes closed

ABSTRACT

Regional homogeneity (ReHo) quantifies spatially local synchronization of resting state fMRI signal and has been applied to lots of clinic studies. Accumulating evidences demonstrated that the synchronization between spatially distinct brain regions, i.e. functional connectivity, can be remarkably influenced if the global mean time course is regressed out, namely global signal regression (GSR). Very recently, it was reported GSR reduces the test–retest reliability of ReHo, and reduces the positive correlation between ReHo and head motion. In this study, we were interested in two questions: 1) how GSR affects the raw ReHo values and its spatial distribution over the brain; 2) how GSR affects the differences of ReHo between two resting states, eyes open (EO) and eyes closed (EC), in healthy individuals. We found that the ReHo values were reduced by GSR but the spatial distribution of ReHo was not changed remarkably. In addition, split-half reproducibility analysis showed reproducible ReHo difference between EO and EC in some areas (e.g., thalamus and caudate) only with GSR, but showed reproducible ReHo difference in some other area (right temporal pole) only without GSR. The effects of GSR were almost independent of regression of other nuisance covariates. Our results suggest that the influences of GSR on ReHo are remarkable, reliable and complex. For the between-condition comparison, the GSR effects are region specific. We suggest that, for application studies using ReHo approach, it would be helpful to report results both with and without GSR.

1. Introduction

Recently, there has been an increasing interest in using functional magnetic resonance imaging (fMRI) to investigate the ongoing neuronal processes at the "resting" state. Most resting state fMRI (rs-fMRI) studies examine the temporal synchronization of the spontaneous brain activities among functional related but usually spatially distinct brain regions [1–5]. However, it has been suggested that the spatially localized synchronization of rs-fMRI signal may also be of functional significance [6–9]. Regional homogeneity (ReHo) [6] is such an approach to measure the synchronization of signal within clusters of nearest neighboring voxels. Several studies have consistently shown that the brain regions with the highest ReHo value are mainly located in the midline regions of default mode network (DMN) [10,11]. These regions are reported to maintain the highest level of regional cerebral blood flow (rCBF) and regional cerebral metabolic rate for oxygen ($rCMRO_2$) in PET study [12]. These results implicated the physiological significance of ReHo may be associated with the magnitude of regional brain activity at rest. To date, the ReHo approach has been widely applied to lots of clinic studies [11,13–16]

Global signal, which is defined as the mean time course of the entire brain, is often considered as an estimation of the global effect which is of no interest [17], and is frequently regressed out from each voxel's BOLD time series in majority of resting state functional connectivity (RSFC) studies [5,18–20]. However, recently global signal regression (GSR) has been demonstrated to have great impact on the RSFC results. For example, several previous studies [18,21–23] showed very similar results of two anti-correlated networks, i.e., default mode network (DMN) and task positive network if GSR was performed, whereas the anti-correlation was not significant [21,22] or weaker [23] when GSR was not performed. Additionally, it has been shown that the distributions of the correlation coefficients are often skewed toward positive in raw resting-state data, but GSR will force this distribution centered on zero [22,23]. It has been found that most voxels correlate with the global signal [23], suggesting that the global signal is more than the simply averaged time series across the whole brain, but represents the global variance which influences

* Corresponding author at: Center for Cognition and Brain Disorders, Hangzhou Normal University, Hangzhou 310015, China. Tel./fax: +86 571 88285651.
E-mail address: charlesliu116@gmail.com (D. Liu).

http://dx.doi.org/10.1016/j.mri.2015.07.011
0730-725X/

the time series of most voxels. Although the validity of GSR in RSFC studies is still under debate [21–27], all the above findings suggest that the global variance in the rs-fMRI data structure has remarkable influence on the RSFC results.

As implicated by the influences of GSR on RSFC results, we reasoned that the ReHo results of rs-fMRI may also be changed if GSR is performed. However, to date only very few studies have investigated the effect of GSR on ReHo. Very recently, it was reported that GSR could reduce the test–retest reliability of ReHo [9], and the positive correlation between ReHo and head motion was reduced by GSR [28]. However, to what extent GSR affects some other key properties of ReHo remains largely unclear.

In the current study, we firstly investigated the influence of GSR on ReHo value and its spatial distribution. Moreover, we wonder whether and to what extent GSR affects the between-group (or between-condition) differences of ReHo. Though ReHo was frequently applied to detect the changes of regional activities in some brain disorders [7,11,13–16] or specific behavior states [6,29,30], little work has considered the impact of GSR. It is very likely that the GSR may exert different influences on ReHo during different resting states, and in turn the ReHo differences would be affected. In this paper, we used a public Eyes-open/Eyes-closed rs-fMRI dataset [30] to examine the influence of GSR on the differences of ReHo between eyes open (EO) and eyes closed (EC) resting states. It has been demonstrated that both the local and the network-based rs-fMRI measurements can be modulated between EO and EC [30–35]. To validate our results, we evaluated the split-half reproducibility of results as did in our previous work [30].

2. Materials and methods

2.1. Participants and data acquisition

The dataset used in this study was from INDI Prospective Data Sharing Samples (http://fcon_1000.projects.nitrc.org/indi/IndiPro.html, Beijing: Eyes open and eyes closed study). Written informed consent was obtained from each participant. There were 48 young healthy participants in this dataset. In the current analysis, three participants were excluded due to incomplete brain coverage. To reduce the potential influence of sample heterogeneity on the reproducibility assessment (see below), we further excluded three non-right-handed participants and two participants with age more than three standard deviations from the mean. Additionally, four more female subjects were excluded to ensure that the two subgroups in the split-half reproducibility analysis were matched for age, gender and session (EO and EC) order. Thus there were 36 subjects remaining (22.2 ± 1.7 years old and 18 males). All the results in this study are based on the data of the remaining 36 participants.

The MR images were acquired using a SIEMENS 3T Trio scanner in the Beijing Normal University Imaging Center for Brain Research. The participants lay supine with the head snugly fixed by straps and foam pads to minimize head movement. Functional images were obtained using an echo-planar imaging sequence with the following parameters: 33 axial slices, thickness/gap = 3.5/0.7 mm, matrix size = 64×64, TR = 2000 ms, TE = 30 ms, flip angle = 90°, FOV = 200×200 mm^2. Each participant underwent three resting state scanning sessions, each lasting for 8 min. Firstly, an EC session was scanned (data of this session were acquired for other purpose and not analyzed in the present study), and then followed by two sessions, EO and EC, with scanning order counter-balanced across participants. During all the rs-fMRI scanning, participants were instructed to keep as motionless as possible, not to think of anything in particular, and not to fall asleep. In addition, a T1-weighted sagittal three-dimensional magnetization-prepared rapid gradient echo (MP-RAGE) sequence was acquired, covering the entire brain: 128 slices, TR = 2530 ms, TE = 3.39 ms, slice thickness = 1.33 mm, flip angle = 7°, inversion time = 1100 ms, FOV = 256×256 mm^2 and matrix size = 256×192.

2.2. Data preprocessing

For each participant's rs-fMRI data at each state (i.e. EO and EC), the first 10 volumes were discarded to make the longitudinal magnetization reach a steady state and for participants to get used to the scanning environment. Slice timing and head motion corrections were firstly carried out. Then fMRI data were spatially normalized to MNI space by three steps: 1) The 3D T1 image was co-registered to the mean motion-corrected functional images. 2) The resulting 3D T1 image was segmented and normalized to Montreal Neurological Institute (MNI) space by using the unified segmentation approach [36] in SPM8. Consequently, a transforming matrix from the original space to MNI space could be obtained for each subject. 3) The transforming matrix was written to the motion-corrected functional images. The functional images were then resampled to $3 \times 3 \times 3$ mm^3. At last, linear trend removing and band-pass (0.01–0.08 Hz) filtering [1] were performed to the data.

2.3. Global signal regression

For each participant and each condition (EO and EC), the global signal was firstly calculated by averaging across all voxels' time courses within a whole brain mask, and then was regressed out from each voxel's time course.

2.4. ReHo calculation

ReHo values were calculated for the data with and without GSR. Accordingly, we termed the results as ReHo-GSR (ReHo with GSR) and ReHo-nGSR (ReHo without GSR) maps. In particular, Kendall's coefficient of concordance (KCC) [37] was calculated to measure the ReHo of each voxel with its spatially nearest neighbors [6]:

$$W = \frac{\sum_{i=1}^{n} (R_i)^2 - n(\overline{R})^2}{\frac{1}{12}K^2\left(n^3 - n\right)} \quad (1)$$

where W is the KCC value which measures the rank correlation among the K time courses. Before calculating ReHo, the time courses were sorted across time, and rank was obtained at each time point for each time course. Then, we calculated R_i as the total rank among the K time courses at the ith time point; $\overline{R}$ is the mean of R_i across all time points. K is the number of voxels within the measured cluster (usually $K = 27$, one center voxel plus the number of its nearest neighbors), and n is the number of ranks (here $n = 230$ time points). The KCC value was assigned to the center voxel of the cubic cluster. Each individual ReHo map was divided by the whole-brain-mean KCC for the standardization purpose [6,28] as was done in the PET study [12] to generate the standardized ReHo maps (mReHo-nGSR maps and mReHo-GSR maps, respectively). Then spatial smoothening with a Gaussian kennel of 6 mm FHWM (full width at half maximum) was performed to individual ReHo (ReHo-GSR and ReHo-nGSR) and mReHo (mReHo-GSR and mReHo-nGSR) maps, respectively.

All the steps above were performed by Data Processing Assistant for Resting-State fMRI (DPARSF, rfmri.org/DPARSF) [38], which is a pipeline data processing toolbox integrating preprocessing modules of Statistical Parameter Mapping (SPM8, www.fil.ion.ucl.ac.uk/spm/) and post-processing modules of REST software (www.restfmri.net) [39].

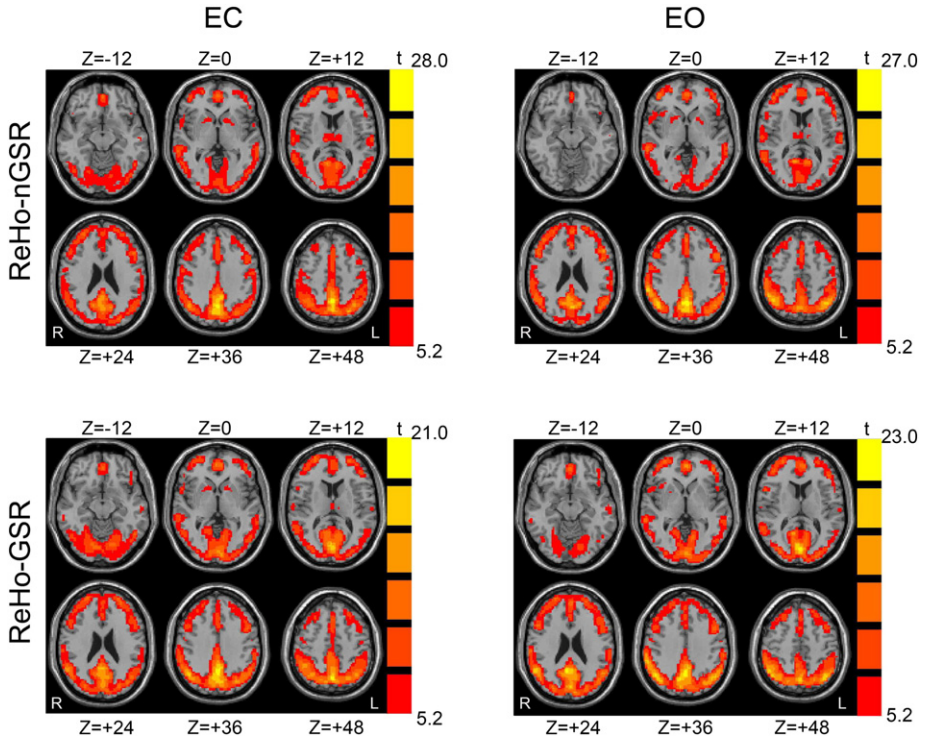

Fig. 1. One-sample t-test results of ReHo-GSR and ReHo-nGSR. The midline regions of DMN had significantly higher ($p < 10^{-5}$, corrected) ReHo values than the whole brain mean, both for ReHo-GSR and ReHo-nGSR, and for both conditions. The left side of the image corresponds to the right side of brain.

2.5. Statistical analyses

2.5.1. Within-condition analyses

It has been consistently revealed that the ReHo value of midline regions of DMN is significantly higher than the whole brain mean KCC [10,11]. We wondered if such spatial distribution of ReHo values was changed by GSR. To this end, we carried out one sided one-sample t-tests on the smoothed mReHo-GSR and mReHo-nGSR maps against 1 (as was done in Ref. [12]). Additionally, we also investigated how the raw ReHo value is affected by GSR. To do this, paired-t test was performed between smoothed ReHo-GSR and ReHo-nGSR maps.

2.5.2. Between-condition analyses

In this section, we investigated the effect of GSR on the differences of ReHo between EO and EC. Particularly, we were interested in whether the GSR could affect the split-half reproducibility of results, which was measured by the spatial overlap of thresholded t-maps of the two halves of the sample. The participants were assigned into two subgroups (we termed them as "Subgroup 1" and "Subgroup 2" in the following) randomly with the constraint that their age, gender and session (EO and EC) order were matched.

Then paired t-tests were carried out to reveal the differences of ReHo between EO and EC in a voxel-wise way, for each subgroup, and for the smoothed mReHo-GSR and mReHo-nGSR maps, respectively. To control Type I error in the resulting statistical maps, we used the AlphaSim program in AFNI [40] software to perform the multiple comparison correction. By iterating the process of random image generation, spatial correlation of voxels, thresholding and cluster identification, the program provides an estimate of the overall significance level achieved for various combinations of individual voxel probability threshold and cluster size threshold [41]. As the result, a contiguity threshold of 228 contiguous voxels and voxel-level $p < 0.05$ were used as criteria for significant difference corresponding to a corrected $p < 0.05$. Then thresholded t-maps of the two subgroups were binarized and combined to generate the overlap maps.

Then, we repeated the above split-half procedure for 1000 times with the two subgroups being randomly re-assigned for each time, while ensuring that their age, gender and scanning orders were matched. Then for each repeat, we performed paired t-tests and constructed the overlap maps in the same way as above. At last, the 1000 overlap maps were added up and divided by 1000 to generate the overlap probability maps. The overlap probability value of each voxel is the ratio of overlap number during the 1000 repeats to the total repeat number (i.e. 1000). Again, all the steps above were carried out on the data with and without GSR, respectively. Of note, the reproducibility assessment is necessary. As the functional significance of both ReHo and GSR is not fully understood, there is great need to evaluate the reproducibility to improve the credibility of conclusions. The aim of repeating the split-half reproducibility assessment for 1000 times is to reduce the errors brought up by single split-half, as in previous work we noticed that the area of overlap regions took only less than 30% of the supra-threshold regions in either subgroup even when conservative threshold was used [30], which suggests large across-subject variability exists.

2.6. Robustness over spatial interpolation methods

Theoretically, ReHo may be sensitive to different spatial interpolation methods during data preprocessing. To test whether our findings are robust over these options, we changed the spatial interpolation methods from the default settings ("4th Degree B-Spline" for motion correction and "trilinear" for spatial normalization) in SPM8 package to "7th Degree B-Spline" for both preprocessing steps. The other analyses kept the same as above. Then we compared the patterns based on different spatial interpolation methods by visual inspection.

2.7. Influences of other nuisance covariates

In RSFC studies, other nuisance covariates including white matter, cerebrospinal fluid (CSF) signals and head motion parameters are usually regressed out to remove the potential variance related to non-neuronal

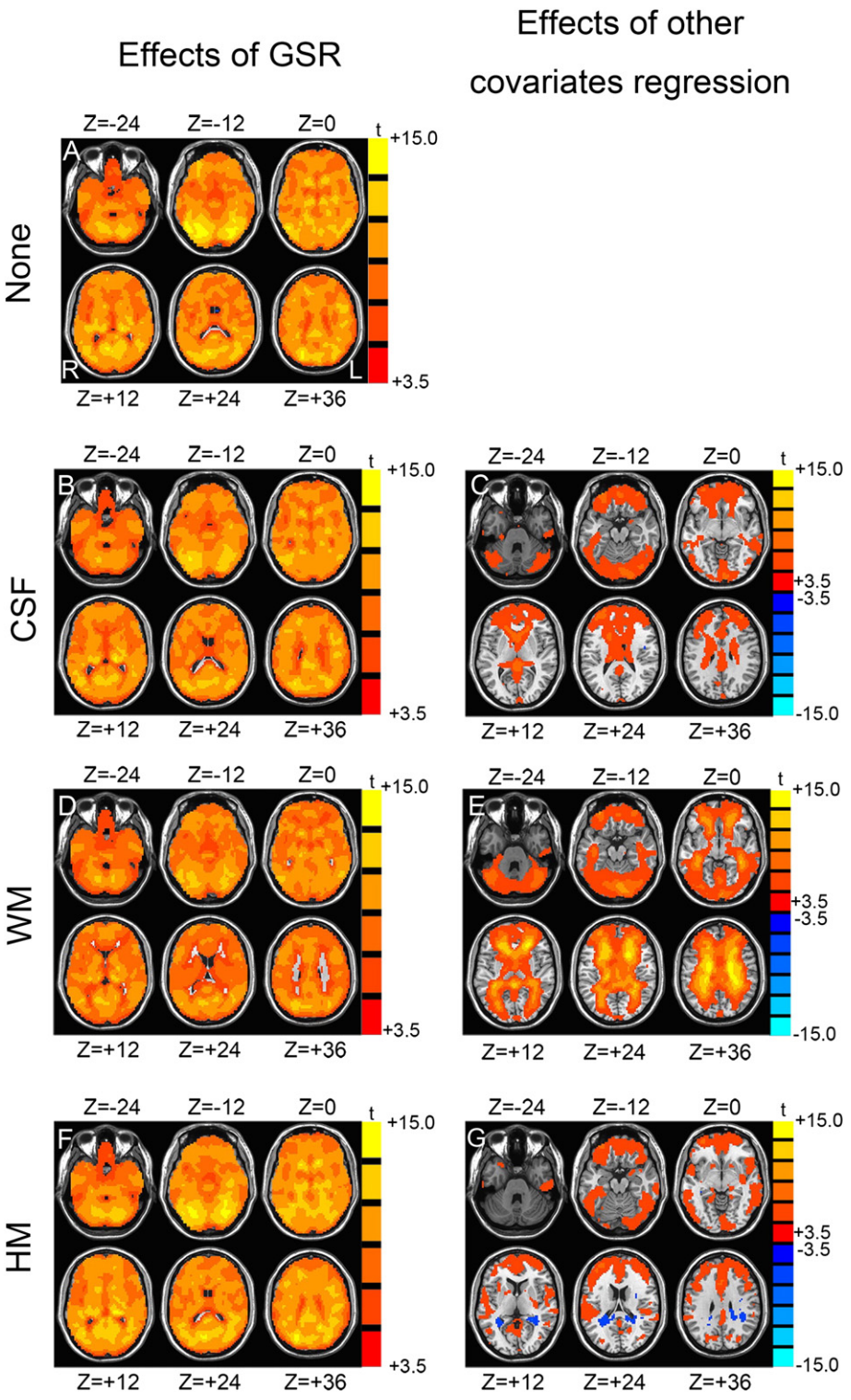

Fig. 2. Influences of nuisance covariates regression on raw ReHo value The left column shows the paired t-test results between ReHo-nGSR and ReHo-GSR, with additional covariates (A, no other covariates, None; B, cerebrospinal fluid signal, CSF; C, white matter signal, CSF; D, head motion parameters, HM) also regressed. The results indicate that ReHo values in most area are significantly ($p < 0.01$, corrected) reduced if GSR is performed. The right column shows the paired t-test results between ReHo-nGSR and ReHo maps with additional covariate (E, CSF; F, WM; G, HM) regression. For the cases of GSR, each of the additional covariates (CSF, WM or HM) was added into the regression model together with the GS. The left side of the image corresponds to the right side of brain.

activities. However, there was not a common strategy for these covariates regression in previous ReHo studies [6,7,9,11,14–16,29]. On the other hand, since these covariates may have contribution to global signal, the effect of GSR on ReHo may be putatively dependent on whether these covariates are regressed out. In this study, we comprehensively assessed the effects of these covariates.

Particularly, WM and CSF ROIs were firstly determined from SPM's a priori template (thresholds: 0.9 for WM and 0.7 for CSF). For the preprocessed data, the averaged signals within these two ROIs were taken as WM and CSF covariates, respectively. The six head motion parameters (x, y, z translations and α, β, γ rotations) obtained during the preprocessing step were taken as HM covariates.

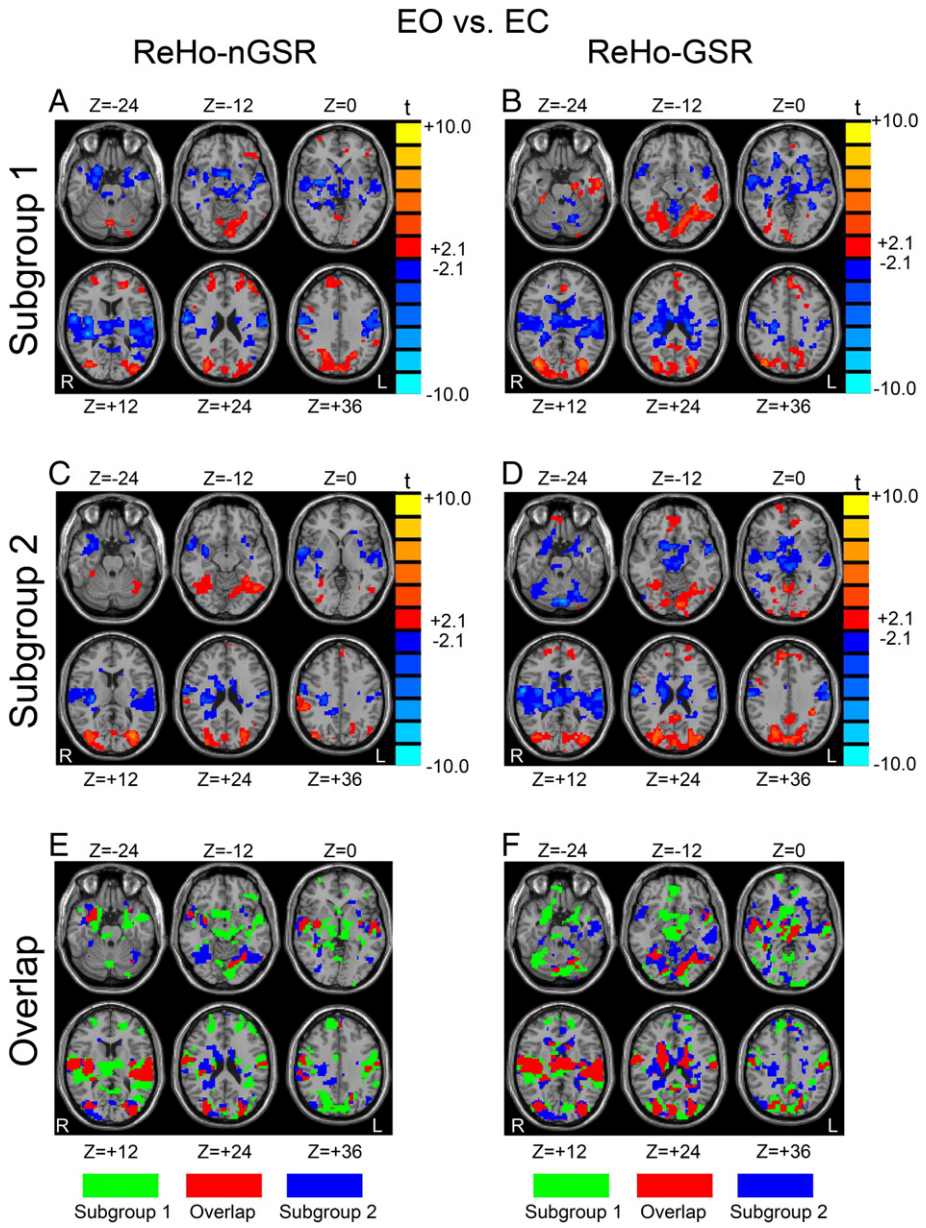

Fig. 3. Paired t-test results between EO and EC for ReHo-nGSR and ReHo-GSR, together with the overlap maps of two subgroups. The first two rows are thresholded t-maps for ReHo-nGSR (A: Subgroup 1 and C: Subgroup 2) and ReHo-GSR (B: Subgroup 1 and D: Subgroup 2). Significant threshold was set at $p < 0.05$ (corrected). The warm color indicates significantly higher ReHo at EO than EC, and the cold color indicates the opposite. The bottom row is the overlap maps between the two subgroups for ReHo-nGSR (E) and ReHo-GSR (F), respectively. The left side of the image corresponds to the right side of the brain.

The effect of each kind of covariate was investigated separately. For the cases with GSR, these covariates were added into the regression model together with the global signal (GS). Then, ReHo calculation and statistical analyses were kept the same as described before.

3. Results and discussion

3.1. Within-condition results

One-sample t-test maps (Fig. 1, $p < 10^{-5}$, corrected) demonstrated that with GSR performed, gray matter in the midline regions of DMN, including PCC/precuneus and medial prefrontal cortex, still had significantly higher ReHo values than the whole brain mean KCC. The pattern was nearly the same with those results without GSR, and those reported in previous ReHo studies [10,11]. These results suggest that the global variance has little impact on the patterns of within-condition ReHo result. Such patterns were also robust with different interpolation methods (Fig. S1), and with other covariates regression (Fig. S4).

Although the patterns of within-condition results were similar between ReHo-GSR and ReHo-nGSR, paired t-tests revealed that GSR reduced the raw ReHo values significantly almost everywhere in the brain (Fig. 2A, $p < 0.01$, corrected). These results were quite in accordance with the previous finding that the global effect has ubiquitous influence on rs-fMRI signal [23]. Different spatial interpolation methods yielded very similar results (Fig. S2). The effects of GSR were still widespread and prominent after other covariates were regressed out (Fig. 2B, D and F).

In contrast to GSR, the influences of other nuisance covariates regression were more spatially restricted (Fig. 2C, E and G).

3.2. Between-condition results

Generally, patterns of the EO-EC differences were quite similar for ReHo-GSR and ReHo-nGSR. Compared to EC, we observed

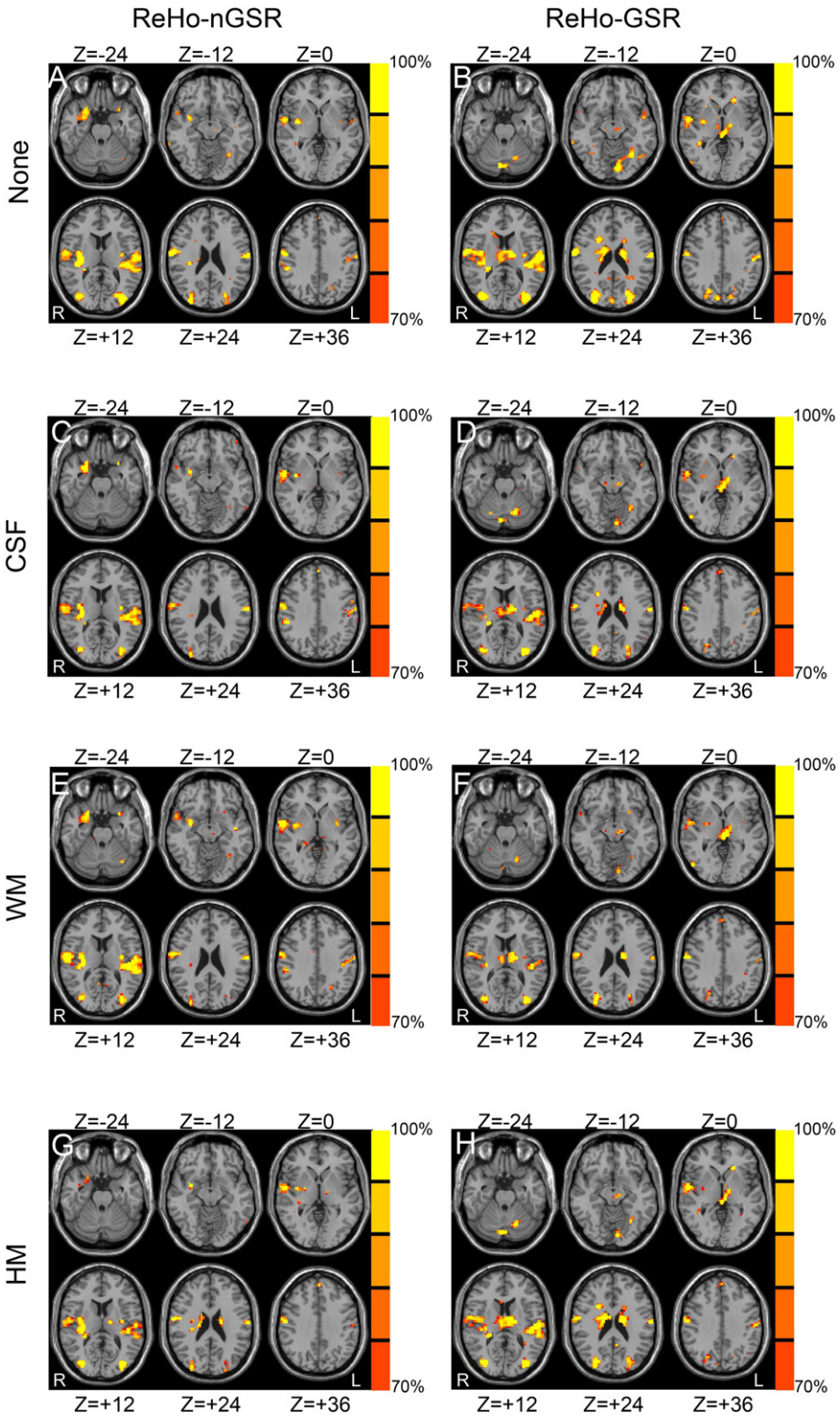

Fig. 4. Overlap probability maps for ReHo-GSR and ReHo-nGSR. The color scheme represents how many times a voxel was identified as overlap across 1000 repeats. The ovarlap probability map was obtained by applying the random split-half procedure 1000 times to the sample and summing up the 1000 overlap maps (see *Methods*). Here we showed those voxels with probability larger than 70%. The left column shows the results without GSR, and the right column shows the results with GSR. Each row shows the results with additional nuisance covariates (None, no other covariates, A and B; WM, white matter signal, C and D; CSF, cerebrospinal fluid signal, E and F; HM, head motion parameters, G and H) regression. For the cases of GSR, each of the additional covariates (CSF, WM or HM) was added into the regression model together with the GS. The left side of the image corresponds to the right side of brain.

significantly increased ReHo in bilateral middle and superior occipital gyrus, fusiform gyrus (FG) and parts of superior prefrontal cortex, and significantly decreased ReHo in primary sensorimotor cortex and auditory cortex at EO condition (Fig. 3, A–D, $p < 0.05$, corrected). This is the case for both ReHo-GSR and ReHo-nGSR.

However, some discrepancy was apparent between the ReHo-GSR and ReHo-nGSR results. First, in lingual gyrus (LG) and its adjacent areas, superior occipital gyrus (SOG) and cuneus, the reliable results (the overlap between subgroups) of ReHo-GSR had larger spatial extent than those of ReHo-nGSR (Fig. 3, E and F). Moreover, only when GSR was performed, EO showed significantly higher ReHo than EC in the thalamus and caudate in both subgroups, but this result could only be seen in one subgroup without GSR (Fig. 3, $p < 0.05$, corrected). In right temporal pole, EO showed significantly higher ReHo than EC in both subgroups only when GSR was not performed and this result was only revealed in one subgroup with GSR performed (Fig. 3, $p < 0.05$, corrected).

The reproducibility of such discrepancy was further confirmed by applying 1000-times split-half procedure to reduce errors. In particular, we defined those regions with more than 700 overlaps out of the 1000 repeats as reproducible. The patterns of the overlap probability maps, based on the 1000 repeated runs, remained quite similar with the overlap maps (Fig. 3). Thalamus, caudate, LG, SOG and cuneus showed more reproducible results only when GSR was performed, and right temporal pole showed more reproducible results only without GSR (Fig. 4A and B).

Generally, the influence of GSR on ReHo differences is more complex than the within-condition ReHo results. For the regions such as thalamus, caudate and several clusters in visual cortex, GSR facilitates the detection of between-condition differences. This may be due to the fact that GSR reduces the shared variance across voxels [21] and thus improves the sensitivity and specificity. In our results, the thalamic cluster found after GSR overlaps to a great extent with the motor/premotor, sensorimotor, and prefrontal subregions of thalamus as revealed in previous DTI studies [42,43]. The cluster of caudate lies in its caudal part, which has strong connections with motor cortex [44]. Previous studies indicated these regions involved in motor control [45–49] and motor learning [50,51]. Therefore, here the role of the two regions may be involved with regulating the ongoing activity of motor cortex between EO and EC (Fig. 3). The decreased local activity of primary sensorimotor cortex between EO and EC was consistently found [30,31,33–35], and may reflect the cross modal inhibition between extrastriate cortex and sensorimotor cortex [52].

We also found the reliable difference in temporal pole only if GSR was not performed. This area was found to be involved in semantic processing [53]. The decreased ReHo in this area, as well as the primary auditory cortex in EO may reflect the cross modal inhibition between visual and auditory cortices [54], i.e. decrease in the ongoing activities of auditory cortex by visual input. Some papers argued that GSR can introduce bias since the signal of interest in some regions may not be orthogonal to the global signal [22,55], thus we speculated that the disappearance of right temporal pole after GSR may be due to such underestimation effect.

For the between-condition results, the discrepancy between ReHo-GSR and ReHo-nGSR was robust with interpolation methods (Fig. S3), and was nearly independent of whether other covariates were regressed out (Fig. 4), suggesting GSR has its unique influence on ReHo than the other covariates regression. Although not so obvious as GSR, regression of other different covariates showed non-negligible effects on ReHo. Particularly, CSF and WM regression reduced the size of reproducible areas for both ReHo-GSR and ReHo-nGSR (Fig. 4C, D, E and F). HM regression showed more influence on ReHo-nGSR than ReHo-GSR (Fig. 4G and H), which indicated that head motion effect may share components with the global signal, and motion effects need to be removed especially when GSR was not applied.

4. Conclusions

The current study demonstrated that the effect of GSR on ReHo (i.e. localized synchronization) of rs-fMRI signal is remarkable, reliable and very complex. For the within-condition results, the raw ReHo values were reduced but the patterns remained nearly unchanged. For the between-condition statistical results, the influence of GSR on ReHo results is region specific. The impact of GSR is nearly independent of regression of other covariates. Future ReHo studies must be interpreted with caution if there is a potential global effect on the issue they concern, especially in some regions like subcortical regions and temporal pole. We would suggest that it would be better for the ReHo application studies to report results of both ReHo-GSR and ReHo-nGSR.

Acknowledgments

Financial support for the data used in this project was provided by grants from the National Natural Science Foundation of China: 81020108022, 81271652, 81201083, 31471084. Dr. Zang is partly supported by “Qian Jiang Distinguished Professor” program.

Supplementary data

Supplementary data to this article can be found online at http://dx.doi.org/10.1016/j.mri.2015.07.011.

References

[1] Biswal B, Yetkin FZ, Haughton VM, Hyde JS. Functional connectivity in the motor cortex of resting human brain using echo-planar MRI. Magn Reson Med 1995;34(4):537–41.
[2] Lowe MJ, Mock BJ, Sorenson JA. Functional connectivity in single and multislice echoplanar imaging using resting-state fluctuations. Neuroimage 1998;7(2):119–32.
[3] Cordes D, Haughton VM, Arfanakis K, Wendt GJ, Turski PA, Moritz CH, et al. Mapping functionally related regions of brain with functional connectivity MR imaging. AJNR Am J Neuroradiol 2000;21(9):1636–44.
[4] Greicius MD, Krasnow B, Reiss AL, Menon V. Functional connectivity in the resting brain: a network analysis of the default mode hypothesis. Proc Natl Acad Sci U S A 2003;100(1):253–8.
[5] Fox MD, Raichle ME. Spontaneous fluctuations in brain activity observed with functional magnetic resonance imaging. Nature reviews. Neuroscience 2007;8(9):700–11.
[6] Zang Y, Jiang T, Lu Y, He Y, Tian L. Regional homogeneity approach to fMRI data analysis. Neuroimage 2004;22(1):394–400.
[7] Li SJ, Li Z, Wu G, Zhang MJ, Franczak M, Antuono PG. Alzheimer disease: evaluation of a functional MR imaging index as a marker. Radiology 2002;225(1):253–9.
[8] Zhang D, Raichle ME. Disease and the brain's dark energy. Nature reviews. Neurology 2010;6(1):15–28.
[9] Zuo XN, Xu T, Jiang L, Yang Z, Cao XY, He Y, et al. Toward reliable characterization of functional homogeneity in the human brain: preprocessing, scan duration, imaging resolution and computational space. Neuroimage 2013;65:374–86.
[10] Long XY, Zuo XN, Kiviniemi V, Yang Y, Zou QH, Zhu CZ, et al. Default mode network as revealed with multiple methods for resting-state functional MRI analysis. J Neurosci Methods 2008;171(2):349–55.
[11] He Y, Wang L, Zang Y, Tian L, Zhang X, Li K, et al. Regional coherence changes in the early stages of Alzheimer's disease: a combined structural and resting-state functional MRI study. Neuroimage 2007;35(2):488–500.
[12] Raichle ME, MacLeod AM, Snyder AZ, Powers WJ, Gusnard DA, Shulman GL. A default mode of brain function. Proc Natl Acad Sci U S A 2001;98(2):676–82.
[13] Cao Q, Zang Y, Sun L, Sui M, Long X, Zou Q, et al. Abnormal neural activity in children with attention deficit hyperactivity disorder: a resting-state functional magnetic resonance imaging study. Neuroreport 2006;17(10):1033–6.
[14] Guo WB, Sun XL, Liu L, Xu Q, Wu RR, Liu ZN, et al. Disrupted regional homogeneity in treatment-resistant depression: a resting-state fMRI study. Prog Neuro-Psychopharmacol Biol Psychiatry 2011;35(5):1297–302.
[15] Paakki JJ, Rahko J, Long X, Moilanen I, Tervonen O, Nikkinen J, et al. Alterations in regional homogeneity of resting-state brain activity in autism spectrum disorders. Brain Res 2010;1321:169–79.
[16] Yuan Y, Zhang Z, Bai F, Yu H, Shi Y, Qian Y, et al. Abnormal neural activity in the patients with remitted geriatric depression: a resting-state functional magnetic resonance imaging study. J Affect Disord 2008;111(2–3):145–52.
[17] Macey PM, Macey KE, Kumar R, Harper RM. A method for removal of global effects from fMRI time series. Neuroimage 2004;22(1):360–6.
[18] Fox MD, Snyder AZ, Vincent JL, Corbetta M, Van Essen DC, Raichle ME. The human brain is intrinsically organized into dynamic, anticorrelated functional networks. Proc Natl Acad Sci U S A 2005;102(27):9673–8.

[19] Wang K, Liang M, Wang L, Tian LX, Zhang XQ, Li KC, et al. Altered functional connectivity in early Alzheimer's disease: a resting-state fMRI study. Hum Brain Mapp 2007;28(10):967–78.
[20] Castellanos FX, Margulies DS, Kelly C, Uddin LQ, Ghaffari M, Kirsch A, et al. Cingulate-precuneus interactions: a new locus of dysfunction in adult attention-deficit/hyperactivity disorder. Biol Psychiatry 2008;63(3):332–7.
[21] Weissenbacher A, Kasess C, Gerstl F, Lanzenberger R, Moser E, Windischberger C. Correlations and anticorrelations in resting-state functional connectivity MRI: a quantitative comparison of preprocessing strategies. Neuroimage 2009;47(4):1408–16.
[22] Murphy K, Birn RM, Handwerker DA, Jones TB, Bandettini PA. The impact of global signal regression on resting state correlations: are anti-correlated networks introduced? Neuroimage 2009;44(3):893–905.
[23] Fox MD, Zhang D, Snyder AZ, Raichle ME. The global signal and observed anticorrelated resting state brain networks. J Neurophysiol 2009;101(6):3270–83.
[24] Anderson JS, Druzgal TJ, Lopez-Larson M, Jeong EK, Desai K, Yurgelun-Todd D. Network anticorrelations, global regression, and phase-shifted soft tissue correction. Hum Brain Mapp 2011;32(6):919–34.
[25] Saad ZS, Gotts SJ, Murphy K, Chen G, Jo HJ, Martin A, et al. Trouble at rest: how correlation patterns and group differences become distorted after global signal regression. Brain connectivity 2012;2(1):25–32.
[26] Scholvinck ML, Maier A, Ye FQ, Duyn JH, Leopold DA. Neural basis of global resting-state fMRI activity. Proc Natl Acad Sci U S A 2010;107(22):10238–43.
[27] Buckner RL. The brain's default network: origins and implications for the study of psychosis. Dialogues Clin Neurosci 2013;15(3):351–8.
[28] Yan CG, Craddock RC, Zuo XN, Zang YF, Milham MP. Standardizing the intrinsic brain: towards robust measurement of inter-individual variation in 1000 functional connectomes. Neuroimage 2013;80:246–62.
[29] Wang DY, Liu DQ, Li SF, Zang YF. Increased local synchronization of resting-state fMRI signal after episodic memory encoding reflects off-line memory consolidation. Neuroreport 2012;23(15):873–8.
[30] Liu D, Dong Z, Zuo X, Wang J, Zang Y. Eyes-open/eyes-closed dataset sharing for reproducibility evaluation of resting state fMRI data analysis methods. Neuroinformatics 2013;11(4):469–76.
[31] McAvoy M, Larson-Prior L, Nolan TS, Vaishnavi SN, Raichle ME, d'Avossa G. Resting states affect spontaneous BOLD oscillations in sensory and paralimbic cortex. J Neurophysiol 2008;100(2):922–31.
[32] Xu P, Huang R, Wang J, Van Dam NT, Xie T, Dong Z, et al. Different topological organization of human brain functional networks with eyes open versus eyes closed. Neuroimage 2014;90:246–55.
[33] Yan C, Liu D, He Y, Zou Q, Zhu C, Zuo X, et al. Spontaneous brain activity in the default mode network is sensitive to different resting-state conditions with limited cognitive load. PLoS One 2009;4(5):e5743.
[34] Jao T, Vertes PE, Alexander-Bloch AF, Tang IN, Yu YC, Chen JH, et al. Volitional eyes opening perturbs brain dynamics and functional connectivity regardless of light input. Neuroimage 2013;69:21–34.
[35] Yang H, Long XY, Yang YH, Yan H, Zhu CZ, Zhou XP, et al. Amplitude of low frequency fluctuation within visual areas revealed by resting-state functional MRI. Neuroimage 2007;36(1):144–52.
[36] Ashburner J, Friston KJ. Unified segmentation. Neuroimage 2005;26(3):839–51.
[37] Kendall MG, Gibbons JD. Rank correlation methods. 5th ed. London: Edward Arnold; 1990[vii, 260 pp.].
[38] Chao-Gan Y, Yu-Feng Z. DPARSF: a MATLAB toolbox for "pipeline" data analysis of resting-state fMRI. Front Syst Neurosci 2010;4:13.
[39] Song XW, Dong ZY, Long XY, Li SF, Zuo XN, Zhu CZ, et al. REST: a toolkit for resting-state functional magnetic resonance imaging data processing. PLoS One 2011;6(9):e25031.
[40] Cox RW. AFNI: software for analysis and visualization of functional magnetic resonance neuroimages. Comput Biomed Res 1996;29(3):162–73.
[41] Ledberg A, Akerman S, Roland PE. Estimation of the probabilities of 3D clusters in functional brain images. Neuroimage 1998;8(2):113–28.
[42] Behrens TEJ, Johansen-Berg H, Woolrich MW, Smith SM, Wheeler-Kingshott CAM, Boulby PA, et al. Non-invasive mapping of connections between human thalamus and cortex using diffusion imaging. Nat Neurosci 2003;6(7):750–7.
[43] Zhang D, Snyder AZ, Shimony JS, Fox MD, Raichle ME. Noninvasive functional and structural connectivity mapping of the human thalamocortical system. Cereb Cortex 2010;20(5):1187–94.
[44] Draganski B, Kherif F, Kloppel S, Cook PA, Alexander DC, Parker GJ, et al. Evidence for segregated and integrative connectivity patterns in the human basal ganglia. J Neurosci 2008;28(28):7143–52.
[45] Marchand WR, Lee JN, Suchy Y, Garn C, Chelune G, Johnson S, et al. Functional architecture of the cortico-basal ganglia circuitry during motor task execution: correlations of strength of functional connectivity with neuropsychological task performance among female subjects. Hum Brain Mapp 2013;34(5):1194–207.
[46] Mostofsky SH, Powell SK, Simmonds DJ, Goldberg MC, Caffo B, Pekar JJ. Decreased connectivity and cerebellar activity in autism during motor task performance. Brain 2009;132(Pt 9):2413–25.
[47] Philp DJ, Korgaonkar MS, Grieve SM. Thalamic volume and thalamo-cortical white matter tracts correlate with motor and verbal memory performance. Neuroimage 2014;91:77–83.
[48] Sommer MA. The role of the thalamus in motor control. Curr Opin Neurobiol 2003;13(6):663–70.
[49] Spraker MB, Prodoehl J, Corcos DM, Comella CL, Vaillancourt DE. Basal ganglia hypoactivity during grip force in drug naive Parkinson's disease. Hum Brain Mapp 2010;31(12):1928–41.
[50] Doyon J, Bellec P, Amsel R, Penhune V, Monchi O, Carrier J, et al. Contributions of the basal ganglia and functionally related brain structures to motor learning. Behav Brain Res 2009;199(1):61–75.
[51] Lehericy S, Benali H, Van de Moortele PF, Pelegrini-Issac M, Waechter T, Ugurbil K, et al. Distinct basal ganglia territories are engaged in early and advanced motor sequence learning. Proc Natl Acad Sci U S A 2005;102(35):12566–71.
[52] Kawashima R, O'Sullivan BT, Roland PE. Positron-emission tomography studies of cross-modality inhibition in selective attentional tasks: closing the "mind's eye". Proc Natl Acad Sci U S A 1995;92(13):5969–72.
[53] Olson IR, Plotzker A, Ezzyat Y. The Enigmatic temporal pole: a review of findings on social and emotional processing. Brain 2007;130(Pt 7):1718–31.
[54] Laurienti PJ, Burdette JH, Wallace MT, Yen YF, Field AS, Stein BE. Deactivation of sensory-specific cortex by cross-modal stimuli. J Cogn Neurosci 2002;14(3):420–9.
[55] Andersson JLR. How to estimate global activity independent of changes in local activity. Neuroimage 1997;6(4):237–44.